

# Exploiting the Reducing Properties of Lignin for the Development of an Effective Lignin@Cu<sub>2</sub>O Pesticide

Cristina Gazzurelli, Mauro Carcelli, Paolo P. Mazzeo, Claudio Mucchino, Antonio Pandolfi, Andrea Migliori, Suvi Pietarinen, Giuliano Leonardi, Dominga Rogolino,\* and Paolo Pelagatti\*

Lignin is a natural polymer produced in huge amounts by the paper industry. Innovative applications of lignin, especially in agriculture, represent a valuable way to develop a more sustainable economy. Its antioxidant and antimicrobial properties, combined with its biodegradability, make it particularly attractive for the development of plant protection products. Copper is an element that has long been used as a pesticide in agriculture. Despite its recognized antimicrobial activity, the concerns derived from its negative environmental impact is forcing research to move toward the development of more effective and sustainable copper-based pesticides. Here a simple and sustainable way of synthesizing a new hybrid material composed of Cu<sub>2</sub>O nanocrystals embedded into lignin, named Lignin@Cu<sub>2</sub>O is presented. The formation of cuprite nanocrystals leaves the biopolymer intact, as evidenced by infrared spectroscopy, gel permeation chromatography, and Pyrolysis-GC analysis. The combined activity of lignin and cuprite make Lignin@Cu<sub>2</sub>O effective against *Listeria monocytogenes* and *Rhizoctonia solani* at low copper dosage, as evidenced by in vitro and in vivo tests conducted on tomato plants.

the 360 000 tons of pesticides sold in the EU in 2018 were inorganic compounds, among which copper ones occupy a relevant position. Moreover, the use of copper is allowed in organic farming where other synthetic pesticides are forbidden. Copper compounds usually adhere to leave surfaces acting as a protective film that slowly release copper ions toxic to pathogens.<sup>[7]</sup> Metal ions release depends on structural characteristics of the plants as well as by the microorganisms or the type of exudates produced by the plant itself.<sup>[8]</sup> Prolonged and frequent applications of copper-based antimicrobials have raised concerns on the possible negative impact on soil biota<sup>[9]</sup> or groundwater contamination.<sup>[5,10,11]</sup> For these reasons, the European Community has recently lowered the annual maximum copper limit from 6 to 4 Kg ha<sup>-1</sup>.<sup>[12]</sup> Hence, there is an urgent need to develop more sustainable pesticides featured by lower copper content. To move in this direction, nanosized Cu-based materials (CuNPs) endowed with antimicrobial activity were developed. Their large surface area-to-volume ratio and higher bioavailability are considered beneficial characteristics that can help to lower the total amount of metal needed for efficient antibacterial/antifungal activity.<sup>[13–15]</sup> Their mechanism of action depends on the nature of the copper compound employed and on many other factors, such as the physical form of the material, the foliar pH, and the method of

## 1. Introduction

Copper is an essential element not only for life<sup>[1,2]</sup> but also for the development of green technologies, such as solar cells and electric vehicles.<sup>[3]</sup> In agriculture, copper has a long standing prominent position as antibacterial agent since its first appearance as Bordeaux mixture in the late 1885.<sup>[4]</sup> Since then, many Cu-based pesticides have been developed to protect crops against diseases.<sup>[5]</sup> Based on Eurostat data,<sup>[6]</sup> about 53% of

C. Gazzurelli, M. Carcelli, P. P. Mazzeo, C. Mucchino, D. Rogolino, P. Pelagatti  
Department of Chemistry  
Life Sciences and Environmental Sustainability  
University of Parma  
P.co Area delle Scienze 17/A, Parma 43124, Italy  
E-mail: dominga.rogolino@unipr.it; paolo.pelagatti@unipr.it



The ORCID identification number(s) for the author(s) of this article can be found under <https://doi.org/10.1002/adsu.202200108>.

© 2022 The Authors. Advanced Sustainable Systems published by Wiley-VCH GmbH. This is an open access article under the terms of the Creative Commons Attribution License, which permits use, distribution and reproduction in any medium, provided the original work is properly cited.

DOI: 10.1002/adsu.202200108

A. Pandolfi  
Res Agraria s.r.l  
Tortoreto Lido TE 64018, Italy  
A. Migliori  
CNR-IMM Sezione di Bologna  
V. Gobetti 101, Bologna 40129, Italy  
S. Pietarinen  
UPM-Kymmene Oyj  
Alvar Aallon katu1, Helsinki FI-00101, Finland  
G. Leonardi  
Green Innovation GMBH  
Grabenweg 68, Innsbruck 6020, Austria  
P. Pelagatti  
CIRCC (Consorzio Interuniversitario di Reattività Chimica e Catalisi)  
Via Celso Ulpiani 27, Bari 70126, Italy

application.<sup>[16]</sup> The mode of action of CuNPs seems in general different from that of Cu<sup>2+</sup>-based compounds. The activity of CuNPs is considered to be due to the production of reactive-oxygen-species (ROS),<sup>[17,18]</sup> while in the presence of cupric ions the membrane depolarization mode seems to prevail.<sup>[19]</sup> However, the use of CuNPs is not devoid of environmental and toxicity issues,<sup>[20–23]</sup> aspects that must be fully addressed for the development of sustainable products.<sup>[24,25]</sup> We have recently reported on the green preparation and antimicrobial activity of an innovative organic–inorganic hybrid material that is composed of lignin (high molecular weight lignin: HMW) and brochantite Cu<sub>4</sub>(OH)<sub>6</sub>SO<sub>4</sub>, hereinafter referred to as HMW@brochantite.<sup>[26,27]</sup> We envisaged that the combination of these two components could reinforce the already known antimicrobial properties of lignin,<sup>[28,29]</sup> leading to a material with better performances in term of antimicrobial profile. HMW@brochantite revealed a high activity against several food-related pathogens as well as bacteria (*E. amylovora*, *X. campestris*) and fungi (*R. solani*, *B. cinerea*, *P. syringae*, *A. solani*) of agronomical interest, at a copper dose much lower than the one usually applied with commercial products.<sup>[27]</sup> Although lignin is a natural and abundant aromatic polymer with interesting biological properties<sup>[30,31]</sup> and low toxicological profile,<sup>[32–34]</sup> most of lignin is nowadays converted into energy by combustion, thus augmenting the amount of CO<sub>2</sub> released in the atmosphere. Hence, HMW@brochantite satisfies two targets required for the development of sustainable agriculture materials: reduction of the use of heavy metals and recycling of an otherwise burnt waste with a circular economy approach.

Here, we present the synthesis and characterization of new materials obtained by reacting HMW and CuSO<sub>4</sub> in different ratios. Exploiting the reducing properties of lignin, coming from its polyphenolic structure, it is possible to obtain a new material composed by HMW and Cu<sub>2</sub>O (cuprite), hereinafter referred to as HMW@cuprite. It is known that also Cu<sub>2</sub>O is endowed of antibacterial properties, then the use of this two-components material turns to be of agronomical interest. The possibility of obtaining the same material starting from lignin already formulated in a sprayable form (commercial UPM Solargro 100) will also be addressed, representing a very useful and easy way to make a green pesticide directly in the field. HMW@cuprite was tested in

in vitro assays against a panel of bacteria and fungi, revealing a promising activity, in particular against *Listeria monocytogenes* and *Rhizoctonia solani*: the use of HMW@cuprite enables a considerable reduction of metal content, if compared to Cu(I) oxide alone. To assess the possibility of application of this new lignin-based material in agriculture, we performed in vivo tests on tomato against *R. solani* and the results are here presented and discussed.

## 2. Results and Discussion

The reduction of the use of copper in the management of plant diseases is one of the goals to be achieved for a more sustainable agriculture. In this direction, the results recently obtained by our group indicate that this requirement can be satisfied by using materials deriving from the combination of technical lignin (HMW) with CuSO<sub>4</sub> in water at neutral pH (HMW@brochantite).<sup>[26,27]</sup> At neutral pH lignin is practically insoluble and the reaction occurs under heterogeneous conditions. The biopolymer acts only as capping agent toward the brochantite crystals, whose dimension can be experimentally controlled, leading to a material with a good antimicrobial profile.<sup>[27]</sup> It is well known that the antibacterial activity of copper is not limited to the +2 oxidation state, but also Cu<sub>2</sub>O, as cuprite, is featured by antibacterial activity. We decided to investigate the possibility of synthesizing a lignin-based material containing Cu<sub>2</sub>O, enlarging the family of the Lignin@Cu pesticides. The reducing properties of lignin are ascribed to the presence of phenolic OH groups that can be oxidized to quinones.<sup>[35]</sup> Lignin induced reduction of metallic salts with formation of metal nanoparticles is well documented for silver,<sup>[36,37]</sup> gold,<sup>[38]</sup> and platinum group metals,<sup>[39]</sup> while in the case of copper, to the best of our knowledge, there is only one report<sup>[40]</sup> where Cu<sup>2+</sup> reduction is observed at 90 °C. Intrigued by the possibility of using milder conditions, we reacted basic water solutions of HMW with different amounts of CuSO<sub>4</sub>·5H<sub>2</sub>O at room temperature. Lignin was solubilized in water at pH = 11 by addition of NaOH under nitrogen, to avoid the formation of sodium carbonate. Different lignin-to-CuSO<sub>4</sub>·5H<sub>2</sub>O weight ratios (20% and 50% w/w referred to the mass of lignin) were applied to isolate two materials with different contents of copper (5% and 13% referred to the mass of lignin, respectively). The

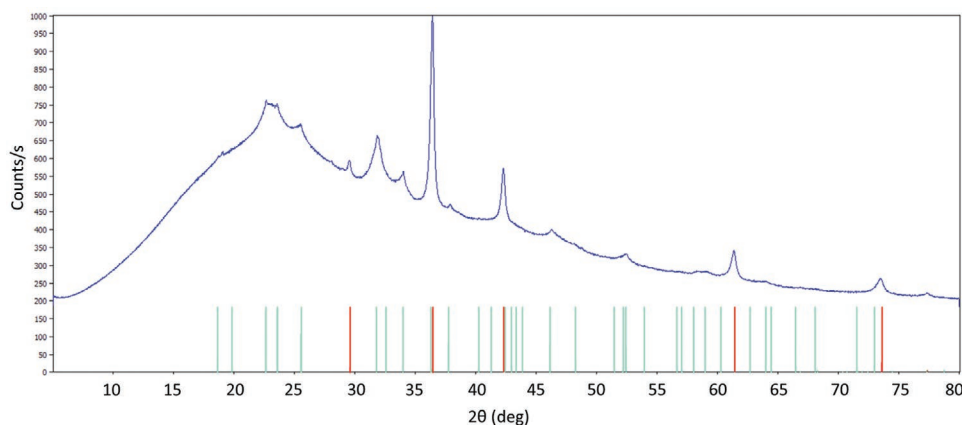


**Figure 1.** XRPD trace of HMW@cuprite (blue line). Red lines correspond to the theoretical  $2\theta$  positions of cuprite Bragg peaks; green lines correspond to the theoretical  $2\theta$  positions of sodium sulfate Bragg peaks, formed as side product during the reaction.

final materials were isolated by evaporation of the solvent and subsequently washed with water. Metal content was determined by inductively coupled plasma (ICP) analysis (Table S1, Supporting Information). X-ray powder diffraction analysis (XRPD) analysis conducted on the new materials gave back different phase compositions depending on the starting amount of copper sulfate. In the case of the sample obtained starting from 5% w/w of Cu, only the peaks belonging to cuprite were found (hereinafter referred to as HMW@cuprite, **Figure 1**), whereas in the sample obtained starting from the higher percentage of metal salt, posnjakite  $\text{Cu}_4(\text{SO}_4)(\text{OH})_6(\text{H}_2\text{O})$  was found as exclusive mineral phase (HMW@posnjakite, Figure S1, Supporting Information). The formation of the two different mineral phases depends on the pH values reached at the end of the copper salt addition. When the pH of the solution was 10.2, HMW@cuprite precipitated, while HMW@posnjakite was exclusively isolated from an acid solution (pH = 5.8). It is known that at room temperature and with  $\text{pH} \leq 10$ , posnjakite is the most favored phase, while at the same temperature but at higher pHs tenorite ( $\text{CuO}$ ) forms.<sup>[41]</sup> The formation of cuprite in place of tenorite must then be ascribed to the reducing ability of lignin. Here, our attention was focused on HMW@cuprite. DLS (dynamic light scattering) analysis conducted on a freshly prepared water dispersion of

HMW@cuprite gave a Z-Average = 184 nm (Figure S2, Supporting Information). The same analysis repeated after 5 days showed a Z-Average = 250 nm, thus highlighting the tendency of the particles to aggregate.

HAADF-STEM (high angle annular dark field-scanning transmission electron microscopy) analysis (**Figure 2**) revealed the presence of  $\text{Cu}_2\text{O}$  nanoparticles, as confirmed by SAED (selected area electron diffraction). EDS (energy dispersive X-ray spectroscopy) analysis conducted on several crystals gave back a semiquantitative Cu/O ratio close to 2/1, in agreement with cuprite composition. The dimensions of the crystals were comprised between 50 and 250 nm. The particle size analysis on a statistical sample of 70 individuals revealed the presence of two populations: one with an average diameter of  $100 \pm 10$  nm and a second with an average diameter of  $200 \pm 10$  nm (Figure 2c), in good agreement with DLS analyses.

To be homogeneously distributed on plants, the product must be properly formulated. To take advantage of the availability of a commercial formulate containing HMW as active ingredient (UPM Solargo 100), we added  $\text{CuSO}_4 \cdot 5\text{H}_2\text{O}$  directly to the formulate. In principle, this procedure allows for the preparation of HMW@cuprite in the field, just before spraying, thus resulting extremely convenient for the final user. Different

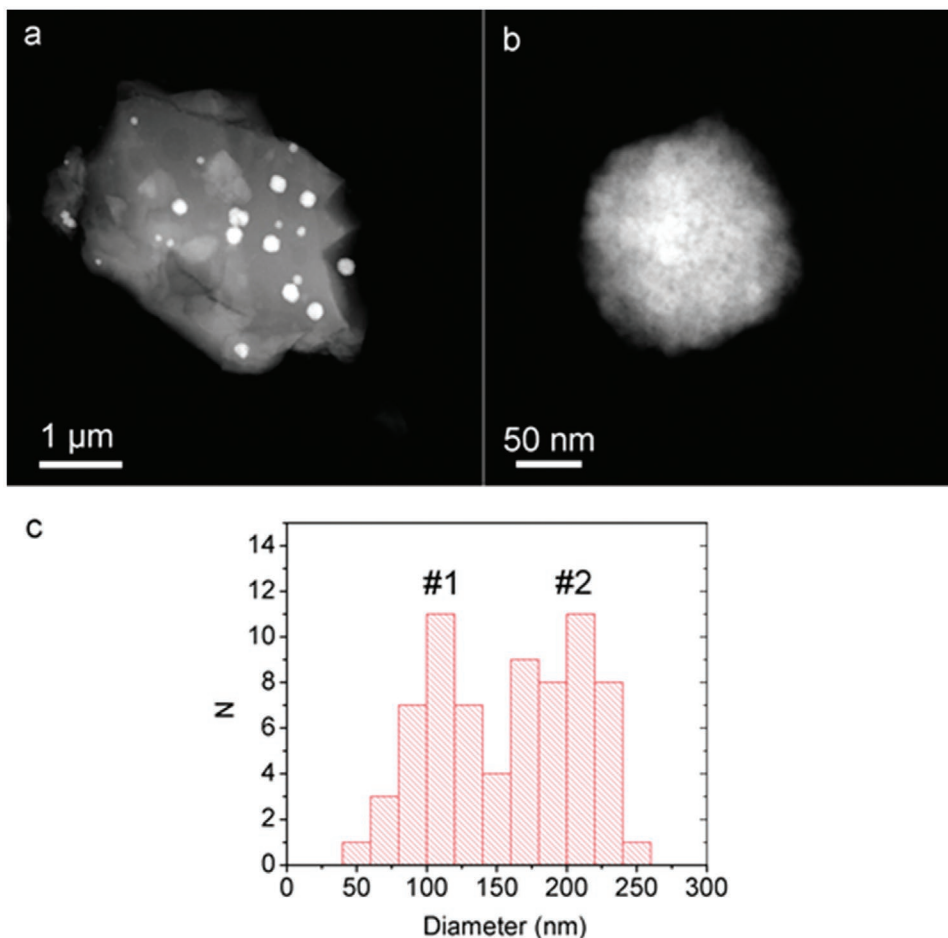


**Figure 2.** TEM analysis of a sample of HMW@cuprite; a) HAADF/STEM image: bright cuprite nanoparticles are well visible among lignin matrix (grey background), b) enlarged view of a cuprite particle, c) particle size distribution histogram showing the presence of two statistical populations.

reactions were conducted between UPM Solargo 100 and  $\text{CuSO}_4 \cdot 5\text{H}_2\text{O}$ , with increasing amounts of salt (5%, 13%, 18% w/w of copper with respect to the lignin contained in the formulate). To note that the pH of UPM Solargo 100 is highly basic ( $\text{pH} > 12$ ). We again chose mild reaction conditions, adding dropwise at room temperature the copper-containing solution into the vigorously stirred formulate. Part of the obtained suspension was withdrawn for DLS analysis (Figure S3, Supporting Information), while the remaining part was dried and analyzed by ICP, XRPD (Table S1 and Figures S4 and S5, Supporting Information) and Transmission Electron Microscopy (TEM). Hereinafter these samples are referred to as  $\text{S\_HMW@phase}_x\%$ , where  $x$  indicates the percentage of copper. The ICP results gave back slightly lower percentages of copper with respect to those expected, especially for  $\text{S\_HMW@cuprite}_5\%$ . This is imputed to the loss of cuprite during the work up, since part of the nanoparticles tend to collect at the bottom of the test tube during centrifugation. Analysis of the XRPD patterns indicated the formation of a mixture of brochantite and cuprite in  $\text{S\_HMW@cuprite/brochantite}_{18\%}$  (Figure S4c, Supporting Information), while cuprite alone was found in the other two samples  $\text{S\_HMW@cuprite}_5\%$  and

$\text{S\_HMW@cuprite}_{13\%}$  (Figure S4a,b, Supporting Information). A higher amount of salt (22% of copper) gave a material containing brochantite and posnjakite ( $\text{S\_HMW@brochantite/posnjakite}$ , Figure S5, Supporting Information), in accord with previous findings.<sup>[26,27]</sup> SAED analysis of  $\text{S\_HMW@cuprite}_5\%$  confirmed the exclusive presence of nanocrystals of cuprite of size ranging between 2 and 5 nm (Figure 3a). These nanocrystals aggregate form spheres of about 50–100 nm. Cuprite was found as exclusive inorganic phase also in  $\text{S\_HMW@cuprite}_{13\%}$  (Figure 3b). Here the size of the crystals range between 2 and 5 nm, with the tendency to aggregate and form clusters of 20–100 nm. A different situation was instead found in  $\text{S\_HMW@cuprite/brochantite}_{18\%}$  (Figure 3c). Here, the aggregates of cuprite nanocrystals are mixed with sticks of brochantite having a length of about 100 nm and a width of about 50 nm. The EDS profiles conducted on the two crystalline phases gave back the expected compositions. The DLS results coming from the initial suspensions were in good agreement with TEM findings (Figure S3, Supporting Information). The results obtained starting from UPM Solargo 100 are of particular interest because in this way it is possible to prepare the target material already formulated and ready to be sprayed on plants.

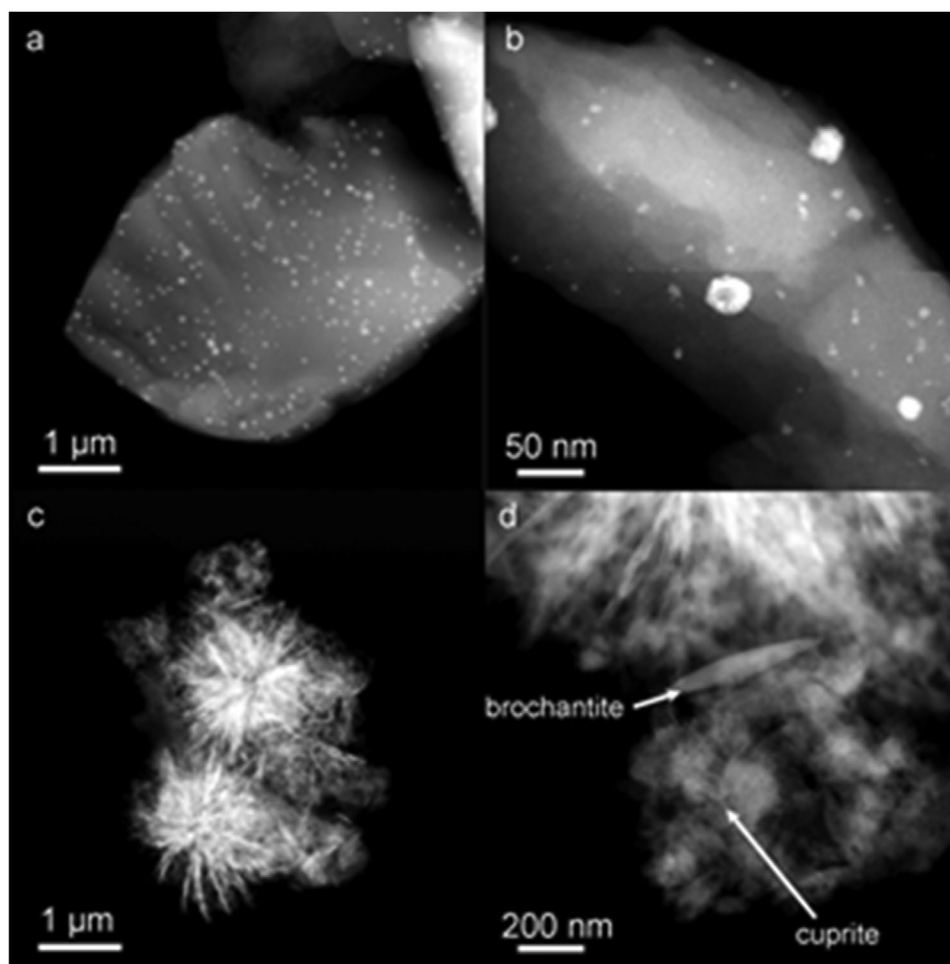


**Figure 3.** HAADF/STEM analysis of a)  $\text{S\_HMW@cuprite}_5\%$ , b)  $\text{S\_HMW@cuprite}_{13\%}$ , c)  $\text{S\_HMW@cuprite/brochantite}$ , d) enlargement to distinguish the crystals of the two different inorganic phases. The bright inorganic nanocrystals are well visible in the lignin matrix (grey background).



**Table 1.** GPC measurements conducted on HMW, HMW@cuprite, HMW@brochantite\_10% (entry 1–3), and HMW and HMW@brochantite\_10% treated with HCl (entry 4, 5).

Entry	Sample	$M_w$ [Da]	$M_n$ [Da]	PI
1	HMW	5959	1560	3.82
2	HMW@cuprite	7066	1662	4.25
3	HMW@brochantite_10% (ref. [27])	7161	1591	4.50
4 <sup>a)</sup>	HMW@brochantite_10%-HCl	5210	1188	4.39
5 <sup>a)</sup>	HMW-HCl	5209	1316	3.96

<sup>a)</sup>HCl 0.02 M, 24 h of stirring.

Since the antimicrobial activity of HMW@cuprite is expected to come from the synergistic effect of the two constituent active phases, it is important to know if the formation of cuprite leads to significant structural changes of the lignin matrix. Hence, an in-depth analysis of the structural features of lignin contained in HMW@cuprite based on gel permeation chromatography (GPC), infrared (IR), thermogravimetric analysis and Pyrolysis-GC/MS analysis was conducted, and the results were compared with untreated lignin HMW.

GPC measurements on both HMW and HMW@cuprite revealed that no fragmentation of lignin occurs during the formation of cuprite nanocrystals.  $M_n$  (number average molecular weight),  $M_w$  (weight average molecular weight) and polydispersity index (PI) of the samples are shown in Table 1. HMW@cuprite presents an  $M_w$  value increased of about 1000 Dalton with respect to starting HMW (Table 1, entries 2 and 1, respectively): this result can be tentatively attributed to an aggregation effect due to the cuprite nanocrystals that lead to the formation of bigger polymeric chain agglomerates.

To test this hypothesis, a GPC analysis was conducted on HMW@brochantite\_10% prepared following our previous synthetic protocol (Figure S7, Supporting Information).<sup>[26]</sup> The same  $M_w$  increase was observed, pointing out that the embedding of inorganic phases into lignin may have such an effect on the  $M_w$  of the polymer. To have a further confirmation, HMW@brochantite\_10% was analyzed after removal of copper by treatment with diluted HCl (Table 1, entry 4). For comparison, the same acid treatment was done also on HMW (Table 1, entry 5). The  $M_w$  values found for the two samples after HCl treatment were very similar, and closer to that of HMW, confirming the aggregating effect of the inorganic phase.

**Table 2.** MIC (Minimum Inhibitory Concentration) values obtained for HMW@cuprite against relevant bacteria and fungi. The metal concentration is shown in brackets.

Microorganism	MIC g L <sup>-1</sup>					
	Lignin	HMW@cuprite	Cu <sub>2</sub> O	Ceftriaxone	Fluconazole	
Bacteria	<i>Staphylococcus aureus</i>	0.78	0.78 (0.027)	0.49 (0.438)	> 64 mg L <sup>-1</sup>	—
	<i>Listeria monocytogenes</i>	3.13	1.56 (0.055)	0.49 (0.438)	8 mg L <sup>-1</sup>	—
	<i>Escherichia coli</i>	3.13	12.50 (0.438)	>1.95 (1.7)	2 mg L <sup>-1</sup>	—
	<i>Xanthomonas campestris</i>	1.56	3.13 (0.109)	1.95 (1.70)	4 mg L <sup>-1</sup>	—
	<i>Pseudomonas syringae pv. actinidiae</i>	1.56	3.13 (0.109)	>1.95 (1.7)	16 mg L <sup>-1</sup>	—
Fungi	<i>Botrytis cinerea</i>	>50	>50	>1.95 (1.7)	—	512 mg L <sup>-1</sup>
	<i>Rhizoctonia solani</i>	0.20	0.02 (0.001)	>1.95 (1.7)	—	16 mg L <sup>-1</sup>

The IR spectra of HMW and HMW@cuprite before washing indicate that the polymer structure is maintained (Figure S6, Supporting Information). The only difference is due to the disappearance of the band at 1705 cm<sup>-1</sup> in the spectrum of HMW@cuprite, related to the stretching of the carboxylic functions.<sup>[42]</sup> This is attributable to the deprotonation of the COOH groups due to the basic conditions under which the reaction was conducted. The peaks at 1121, 635, and 622 cm<sup>-1</sup>, not present in the spectrum of HMW, are instead attributable to Na<sub>2</sub>SO<sub>4</sub> formed as byproduct of the synthesis. Pyrolysis-GC/MS analysis for both HMW and HMW@cuprite are reported in the Supporting Information (Figure S8, Supporting Information).

No significative changes were found in the gaschromatographic profiles of the most characteristic volatiles (Figure S8, Supporting Information).

## 2.1. In Vitro Antimicrobial Activity

Inspired by our previous results obtained with the lignin-based hybrid material HMW@brochantite,<sup>[26,27]</sup> we tested HMW@cuprite against some bacteria (*Staphylococcus aureus*, *Listeria monocytogenes*, *Escherichia coli*, *Xanthomonas campestris*, *Pseudomonas syringae pv. actinidiae*) and fungi (*Botrytis cinerea*, *Rhizoctonia solani*). Cuprite nanoparticles could provide for different antimicrobial profile and/or different solubility, and consequently different release over time with respect to brochantite or posnjakite. Results are collected in Table 2. Fluconazole (against fungi) and Ceftriaxone (against bacteria) were used as positive controls, while copper(I) oxide, often used as commercial fungicide on crops, was considered for comparison as a copper-containing antibacterial and antifungal agent. Copper content (g L<sup>-1</sup>) is given in parentheses. Generally, lignin alone shows a clear inhibitory effect and all strains tested, except *Botrytis cinerea*, are inhibited at relatively low concentrations. It is worth noting that in all cases, except with *B. cinerea*, HMW@cuprite presents interesting minimum inhibitory concentration (MICs) with a copper content ranging from 4 to more than 10<sup>3</sup> times lower than copper(I) oxide alone (Table 2). Worthy of note is that even when MICs of HMW@cuprite are higher than the MIC values found with lignin or Cu<sub>2</sub>O alone (*S. aureus*, *E. coli*, *X. campestris*, *P. syringae*), the inhibition of the microbial growth is obtained with a copper content lower with respect to Cu<sub>2</sub>O. The most interesting data are obtained with *Rhizoctonia*

**Table 3.** The different treatments on “Kero” variety of tomatoes against *R. solani*.

Entry	Code	Composition	Active ingredient	Dosage rate [ha]	Notes
1		Untreated Check	—	—	
2		COPRANTOL 30 WG	Copper oxychloride	1.65 kg ha <sup>-1</sup>	
3		UPM Solargo 100	Lignin	20 L ha <sup>-1</sup>	
4		UPM Solargo 100	Lignin	10 L ha <sup>-1</sup>	
5		Copper Sulfate	CuSO <sub>4</sub> 5H <sub>2</sub> O	200 g ha <sup>-1</sup>	
6	S_HMW@cuprite_5%	UPM Solargo 100	Lignin	10 L ha <sup>-1</sup>	a)
		Copper sulfate	CuSO <sub>4</sub> 5H <sub>2</sub> O	200 g ha <sup>-1</sup>	a)
7	S_HMW@cuprite_13%	UPM Solargo 100	Lignin	4 L ha <sup>-1</sup>	a)
		Copper sulfate	CuSO <sub>4</sub> 5H <sub>2</sub> O	200 g ha <sup>-1</sup>	a)
8	S_HMW@cuprite/brochantite	UPM Solargo 100	Lignin	2.8 L ha <sup>-1</sup>	a)
		Copper sulfate	CuSO <sub>4</sub> 5H <sub>2</sub> O	200 g ha <sup>-1</sup>	a)
9	S_HMW@posnjakite/brochantite	UPM Solargo 100	Lignin	2.2 L ha <sup>-1</sup>	a)
		Copper sulfate	CuSO <sub>4</sub> 5H <sub>2</sub> O	200 g ha <sup>-1</sup>	a)
10	S_HMW@cuprite_2.5%dil	UPM Solargo 100	Lignin	20	b)
		Copper sulfate	CuSO <sub>4</sub> 5H <sub>2</sub> O	200	b)
11	S_HMW@cuprite_5%dil	UPM Solargo 100	Lignin	10	b)
		Copper sulfate	CuSO <sub>4</sub> 5H <sub>2</sub> O	200	b)
12	S_HMW@cuprite_13%dil	UPM Solargo 100	Lignin	4	b)
		Copper sulfate	CuSO <sub>4</sub> 5H <sub>2</sub> O	200	b)

<sup>a)</sup>On-time mixing of UPM Solargo 100 and CuSO<sub>4</sub> 5H<sub>2</sub>O solubilised in a minimum amount of water and subsequent dilution in the tank before spraying. Final volume: 40 L;

<sup>b)</sup>Preliminary dilution of both UPM Solargo 100 (20 L of water) and CuSO<sub>4</sub> 5H<sub>2</sub>O (1 L of water) and subsequent mixing. Final volume: 40 L.

*solani*, where it is evident a strong synergistic effect of lignin with copper. In particular, the MIC of HMW@cuprite corresponds to a copper concentration 1700 times lower than in the case of Cu<sub>2</sub>O alone. Regarding the bacteria, the trial with *Listeria monocytogenes* is also very promising. Toward this microorganism HMW@cuprite exhibits a greater inhibition compared to both lignin and Cu<sub>2</sub>O alone, suggesting a synergistic effect also in this case. Again, the copper content is much lower (about 8 times) with respect to the metal content of the oxide alone. Overall, the in vitro results confirmed the potential of lignin-based material as antibacterial and antifungal agent. In particular, HMW@cuprite shows an excellent selectivity toward *Listeria monocytogenes* and *Rhizoctonia solani*, with a considerable reduction of metal content compared to Cu(I) oxide.

## 2.2. Trials on Crops in the Field

To assess possible applications of HMW@cuprite in agriculture, we performed preliminary tests on crops in the field, by using the “Kero” variety of tomato. Since promising in vitro results were obtained against *Rhizoctonia solani*, we chose to test the efficacy of HMW@cuprite against this wide host range plant pathogen. With the idea to exploit a simple application method, we mixed the commercially available UPM Solargo 100 and copper sulfate just before spraying on leaves: the combination of formulated lignin with copper sulfate generates in situ different Lignin@Cu materials according to the metal to lignin ratio employed, as already discussed in Section 2.1. The different treatments on “Kero” variety of tomatoes against *R. solani* are

reported in Table 3. Two different operational approaches were performed: for entries 6–9, UPM Solargo 100 and copper sulfate, dissolved in the minimum quantity of water, were mixed and subsequently diluted until the final volume was reached (40 L); for entries 10–12 (S\_HMW@cuprite\_X%dil, X = 2.5, 5, 13), both UPM Solargo 100 and copper sulfate were first diluted (in 20 and 1 L of water, respectively) and subsequently mixed and then the final volume was reached (40 L, see Table S4 for details, Supporting Information). Note that, to further explore the role of cuprite, we also used a metal to lignin ratio corresponding to 2.5% copper content with respect to the mass of lignin (entry 10 in Table 3). Incidence (percentage of attacked plants), severity (average attacked area per plant), yield per plot at harvest, vigor of plants, content of chlorophyll, water, and nitrogen of leaves were evaluated at defined intervals (see the Experimental Section for details). A preventive application (application A) of tested compounds was carried out, followed by six applications (applications B–G) at about 7–8 days of interval (Table S4, Supporting Information). To note that the concentration of copper was kept constant (50 g ha<sup>-1</sup>) for all trials. A good level of disease was assessed on the trial area and Table S5 (Supporting Information) collects data about % of incidence and severity for the assessments 7DA-A, 7DA-D, 7 DA-G, and 14 DA-G (DA: days after). Assessments on vigor and content of chlorophyll, water, and nitrogen on leaves did not show significant differences among treatments and no phytotoxicity was observed on any visit and on any treated plot. Efficacy results 7 days after application D (7 DA-D) and 7–14 days after last application G (7DA-G, 14DA-G) are reported as graphs (Figures 4 and 5). All treatments provided significant disease

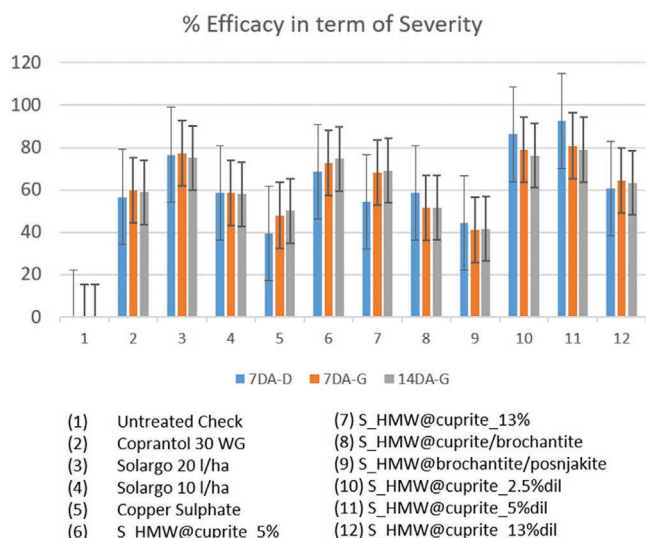


**Figure 4.** Efficacy in terms of severity of attack of treatments against *Rhizoctonia solani* on tomato (variety: “Kero”), with untreated check set as 0%. 7DA-D: 7 days after application D; 7DA-G: 7 days after application G; 14DA-G: 14 days after application G. Standard deviations are reported as bars.

control compared to the untreated check (set as zero). UPM Solargo 100 applied alone at both dosages (20 and 10 L ha<sup>-1</sup>) showed good efficacy compared to the untreated check and a dose-response was also evident. The higher dosage (20 L ha<sup>-1</sup>) appeared generally better than the reference products Coprantol WG (165 g ha<sup>-1</sup>) and copper sulfate (200 g ha<sup>-1</sup>) applied alone (Figures 4 and 5). All the Lignin@Cu materials showed a good efficacy when compared to the reference products Coprantol WG and copper sulfate both in terms of incidence and severity. For both the parameters evaluated, a good performance was

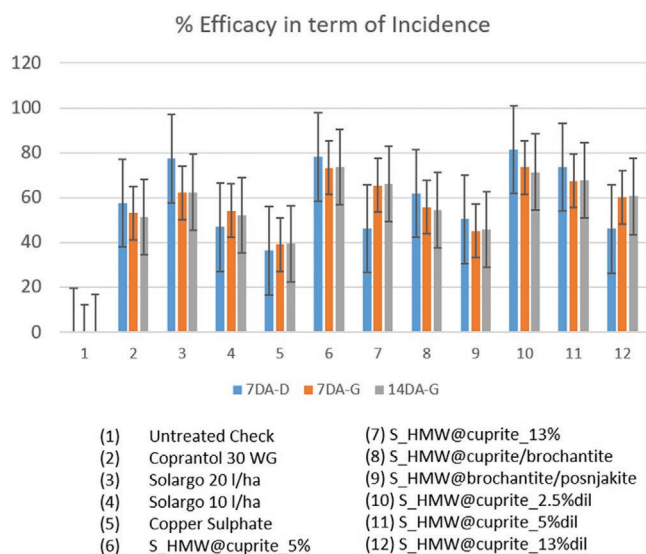


**Figure 5.** Efficacy in terms of incidence of attack of treatments against *Rhizoctonia solani* on tomato (variety: “Kero”), with untreated check set as 0%. 7DA-D: 7 days after application D; 7DA-G: 7 days after application G; 14DA-G: 14 days after application G. Standard deviations are reported as bars.

observed when cuprite was the inorganic phase (entries 6, 7, 10–12), while a decreased efficacy was observed in the presence of brochantite/posnjakite (entries 8 and 9). A dependence on the dose of lignin employed was also evident, the best performance being observed with S\_HMW@cuprite\_5%, S\_HMW@cuprite\_2.5%dil, and S\_HMW@cuprite\_5%dil (entries 6, 10, 11). At the same concentration of copper (50 g ha<sup>-1</sup>), therefore, HMW@cuprite showed a synergic effect offered by the presence of lignin and cuprite, boosting the efficacy on pest control ensured by UPM Solargo 100 and copper sulfate alone, confirming a better profile versus a copper-based pesticide like Coprantol WG.

The best results in terms of incidence and severity were obtained by diluting both UPM Solargo 100 and copper sulfate before their mixing (entries 10 and 11), confirming that 2.5% and 5% of Cu are optimal against *R. solani* in the field. The assessment on yield (Figure 6) generally confirmed the results of efficacy assessment. All treatments showed in fact an improvement versus the untreated check. However, while comparable yields (about 60%) were observed using Coprantol WG, copper sulfate, UPM Solargo 100 alone at both dosages, or when brochantite/posnjakite were the inorganic phases (entries 3–6, 9, and 10), an evident enhancement in terms of yield was registered with S\_HMW@cuprite\_X%, the optimal percentage yield (about 75%) being reached with S\_HMW@cuprite\_2.5% (entry 10).

### 3. Conclusion

Climate changes, issues about environment contamination and resources consumption can no longer be ignored, and research is trying to give new insights for efficient waste management and sustainability in the agricultural field. Our work is aimed to explore the potential of lignin, actually discharged as a waste by bio refineries and pulp industry, as a natural pesticide, which biocidal profile can be synergically boost by the presence of a

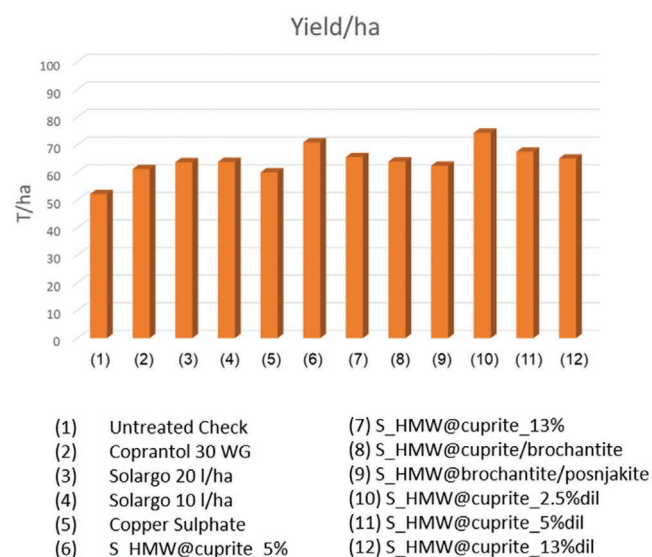


**Figure 6.** Yield/ha reported obtained by assessment on weight of harvestable fruits per plot performed 35 days after the last application.

copper-based inorganic phase.<sup>[25,26]</sup> To note that lowering the copper content with respect to actual commercial pesticides is one important goal to reduce soil and water contamination as well as to defend environmental biota. These aspects are fully consistent with the Sustainable Developing Goals (SDGs) adopted in 2015 by the United Nations, in particular with SDG2 (Sustainable Agriculture), SDG 13 (Climate Change), and SDG 15 (Forests). We have demonstrated that, according to the different metal to lignin ratio, it is possible to tune not only the metal content, but also the type of inorganic phase present in Lignin@Cu materials. Thanks to the reducing properties of lignin, HMW@cuprite can be obtained with a copper content up to 5% referred to the mass of lignin, while HMW@brochantite or HMW@brochantite/posnjakite are obtained with higher metal contents. HMW@cuprite is also formed when a formulated lignin (UPM Solargo 100) is used. In this case higher metal contents can be reached (up to 13% vs the mass of lignin). HMW@cuprite has demonstrated very good efficacy in *in vitro* tests, in particular against *Listeria monocytogenes* and *Rizoctonia solani*, ensuring promising MICs at lower copper contents versus Cu<sub>2</sub>O alone. Evidently, the most interesting results come from preliminary tests conducted on tomatoes against *R. solani*. The Lignin@Cu materials can be easily prepared *in situ* and directly sprayed on leaves: HMW@cuprite confirmed to have the most interesting antifungal profile, ensuring an efficient pest control, better than Coprantol 30 WG and lignin alone. Furthermore, an increase in yield/ha has also been registered (up to 25% with respect to untreated check) when S\_HMW@cuprite\_2.5%dil is employed. Overall, this particular lignin@Cu hybrid material is worth of further investigations for the development of a lignin-based pesticide endowed with good efficacy, particularly in the direction of the understanding of its mechanism of action. This aspect, together with the elucidation of the potential risks for human health associated with the use of nanopesticides, is crucial for the progress of a more sustainable agriculture, and is currently under investigation in our laboratories. At present, there is no doubt that the low metal content and the high efficacy combined with the possibility of recycling a waste, make Lignin@Cu material highly attractive in a circular economy scenario.

#### 4. Experimental Section

**Materials and Methods:** The technical lignin employed in this work (Kraft lignin) is referred to as HMW, while the different copper containing materials, generally indicated as Lignin@Cu, will be referred to as HMW@cuprite (cuprite: Cu<sub>2</sub>O), HMW@posnjakite (posnjakite: Cu<sub>4</sub>(OH)<sub>6</sub>SO<sub>4</sub>·H<sub>2</sub>O), and HMW@brochantite (brochantite: Cu<sub>4</sub>(OH)<sub>6</sub>SO<sub>4</sub>). HMW lignin (BioPiva395; *Pinus taeda*,  $M_w = 5950\text{--}6000\text{ g mol}^{-1}$ ;  $M_n = 1560\text{--}1565$ ) and formulated lignin (UPM Solargo 100) were kindly provided by UPM-Kymmene Oyi (Helsinki, Finland) and Green Innovation GmbH (Innsbruck, Austria). UPM Solargo 100 is a water dispersible liquid solution that contains 100 g L<sup>-1</sup> of hydrolyzed lignin in hydro-glycolic solution (propylene glycol) alkalinized by KOH. CuSO<sub>4</sub>·5H<sub>2</sub>O and NaOH were purchased from Sigma-Aldrich and used with no further purification. Degassed water was obtained by cooling under a stream of nitrogen a previously boiled volume of deionized water. pH was measured using a Crison pHmeter basic 20 equipped with an Ag/AgCl electrode.

**General Procedure for the Synthesis of Lignin@Cu Materials:** A 50 mL two necked round bottom flask equipped with a magnetic bar was

charged with 100 mg of HMW and 5 mL of oxygen-free deionized water. Under stirring, 350 μL of a 1 M NaOH solution were added, and stirring was maintained until complete lignin dissolution (pH = 11). Then, 10 mL of a solution containing CuSO<sub>4</sub>·5H<sub>2</sub>O (20 and 50 mg, corresponding to a Cu content referred to the mass of lignin employed of 5% and 13%, respectively) was added dropwise under a gentle flux of nitrogen. This was necessary to avoid the formation of large amounts of sodium carbonate. The pH of the solution after addition of the salt was 10.2 and 5.8, respectively. After about 5 min from the complete addition of the metal salt, the solution was warmed at 50 °C and water was removed by nitrogen stream under continuous stirring until the isolation of a brown powder. The powder was subsequently washed with water by centrifugation and dried again at 50 °C. The characterization revealed the presence of cuprite (Cu<sub>2</sub>O) in the sample corresponding to a lignin/salt weight ratio of 5 (HMW@cuprite) and posnjakite (Cu<sub>4</sub>(OH)<sub>6</sub>SO<sub>4</sub>·H<sub>2</sub>O) in the sample corresponding to a lignin/salt weight ratio of 13 (HMW@posnjakite).

**Synthesis of Lignin@Cu Materials Starting From UPM Solargo 100:** In a 100 mL Erlenmeyer flask, equipped with a magnetic stirrer, 50 mL of UPM Solargo 100 (corresponding to 5 g of lignin) were added. Under stirring, a solution containing CuSO<sub>4</sub>·5H<sub>2</sub>O was added dropwise (1, 2.6, or 3.5 g, corresponding to a Cu content referred to the mass of lignin employed of 5%, 13%, and 18%, respectively). When the addition of the metal salt was complete the mixture was left stirring for 10 min. Part of the suspension was withdrawn for DLS analysis (see the Supporting Information), while the rest of the suspension was dried at 120–130 °C. Subsequently, the lacquered solid was washed with water, isolated by centrifugation and dried again to obtain a brown powder.

The characterization revealed the presence of cuprite (Cu<sub>2</sub>O) in the first two samples (S\_HMW@cuprite) and a mixture of brochantite and cuprite in the last one (S\_HMW@cuprite/brochantite). S\_HMW@cuprite\_X%dil (X = 2.5%, 5%, 13%) were obtained directly *in situ* for crop trials by diluting UPM Solargo 100 and CuSO<sub>4</sub>·5H<sub>2</sub>O separately (in 20 and 1 L of water, respectively, accordingly to the salt to lignin mass ratios reported in Table S4, Supporting Information) and then mixing. Finally, water was added to reach the final volume (40 L).

**Acid Treatment of HMW and HMW@brochantite:** 1 g of material was dispersed in 200 mL of a 0.01 M HCl solution for 24 h under stirring at room temperature. Subsequently, the solid was filtered and washed with abundant water, then dried at 40 °C for 12 h.

**Characterization of the Materials:** The copper content of the materials was determined by ICP-AES analysis (ICP-Atomic Emission Spectroscopy) by means of a JY 2501 of the HORIBA Jobin Yvon, ULTIMA 2 model, following the procedure already reported<sup>[26]</sup> (see the Supporting Information for details). The mineral phase was identified by XRPD. Data were collected in Bragg–Brentano (BB) geometry with a Cu K<sub>α</sub> radiation on a Rigaku SmartLab XE diffractometer equipped with a solid state HyPix3000 2D detector. To increase the limit of detection (LoD) of any crystalline impurity, data were collected overnight at high counting statistic with 5° Soller slits and variable vertical slits, which guarantee the same volume of sample under the beam along the measurement. Data were then normalized to the counting time. To evaluate the content of the materials, Pawley refinements were performed against cell parameters reported in the literature. TEM characterizations were carried out using a FEI TECNAI F20ST microscope operating at 200 kV and equipped with an EDAX PV9761-SUTW EDS. Scanning transmission (STEM) pictures were recorded using a HAADF detector: in this imaging mode, the intensity I of an image point is proportional to Z<sup>1.7</sup>t, where Z is the mean atomic number and t is the thickness of the specimen. The specimens were prepared by grinding the powders in isopropyl alcohol. The solution was subsequently sonicated for 15 min and drop casted on a holey carbon film heated at 50 °C.

DLS analysis were conducted on HMW@cuprite, S\_HMW@cuprite\_5%, and S\_HMW@cuprite/brochantite samples by means of a Malvern Zetasizer Nano ZSP. Each sample was diluted with deionized water and then subjected to the measure.

**Characterization of the Materials—Gel Permeation Chromatography:** Solid lignin samples were dried in the oven at 60 °C overnight prior



to dissolve about 10–12 mg in 10 mL of a 0.1 M NaOH solution, then filtered with 0.2 µm nylon high performance liquid chromatography filter. Measures were conducted in duplicate by means of Thermo Scientific DIONEX UltiMate 3000 equipped with two detectors: a refractive index detector (RefractoMax520) and a UV detector (Dionex Ultimate 3000 diode array detector at 280 nm). The columns were PSS MCX analytical 1000 and 100 000 Å and a 0.1 M NaOH solution was used as eluent. The system operated at a flow rate of 0.5 mL min<sup>-1</sup> and 30 °C. The measurements were conducted with isocratic run for a run time of 50 min. Calibration was done for UV-detector (280 nm): The PSS-standard, poly(styrenesulfonate)sodium salt, is used with different molar mass (65 400, 29 500, 15 800, 6430, and 891 Da). Standard samples were dissolved to ultrapure water with a concentration of 5 mg mL<sup>-1</sup> and injection volume 20 µL.

**Infrared Spectroscopy (IR):** IR spectra were collected on dried samples with a Thermo Fisher Scientific Nicolet 6700 Fourier transform-infrared, attenuated total reflectance spectrometer equipped with diamond crystal (4000–500 cm<sup>-1</sup> interval)

**Pyrolysis-GC/MS:** Lignin pyrolysis was carried at 600 °C temperature using Frontier Lab pyrolyzer EGA/Py-3030D connected to an Agilent GC/MS-system consisting of 7890B GC and 5977A MSD. The separation column was a HP-5 ms capillary column (30 m, 250 µm inner diameter and 0.25 µm film thickness). GC-parameters: injector temperature 250 °C, split ratio 1:20, oven program starting from 70 °C with 4 min isothermal and continuing with a heating rate of 10 °C min<sup>-1</sup> until finishing with a 20 min hold time at 300 °C final temperature. The transfer line temperature of MS was 300 °C, scan range 40–550 m z<sup>-1</sup> and the ionizing voltage 70 eV. Agilent Chemstation Software was used for instrument control and data processing. Compounds generated in pyrolysis were identified by comparing the MS-spectra against commercial MS-libraries (Wiley and NIST).

**In Vitro Antimicrobial Activity:** The evaluation of the antimicrobial activity was conducted by applying an agar dilution method (CLSI protocol-Clinical and Laboratory Standard Institute)<sup>[43]</sup> to determine the minimum inhibitory concentrations (MICs) of the tested compounds. The assay was performed into 24-well plates with 2 mL of medium. Tested compounds were incorporated at different concentrations into the agar medium (specific to each microorganism) at 55 ± 5 °C and, after solidification of the medium, the inoculum (10<sup>4</sup> CFU mL<sup>-1</sup> for the fungi and 10<sup>5</sup> CFU mL<sup>-1</sup> for the bacteria) was applied to the agar surface. Concentrations of the tested compounds were obtained by making serial dilutions of the presolidified agar suspension at 55 °C; Resulting suspensions were then distributed into the wells and let solidify. Positive controls of antimicrobial activity were used: Fluconazole (against fungi) and Ceftriaxone (against bacteria). All the tests were carried out in triplicate. Minimum inhibitory concentration (MIC, g L<sup>-1</sup>) of tested compounds were determined for each pathogen, and results are summarized in Table 2. *Staphylococcus aureus*, *Listeria monocytogenes*, *Escherichia coli*, *Xanthomonas campestris*, *Pseudomonas syringae* pv. *Actinidiae*, *Botrytis cinerea*, and *Rhizoctonia solani* were tested. Table S1 (Supporting Information) reports the microorganisms with relative specific growth media and conditions used. For each microorganism the following controls were included

- Positive control of growth: microorganisms were plated in agar medium in absence of the compounds
- Control of sterility: the microorganism was not inoculated into the agar medium
- Control of antimicrobial activity: microorganisms were plated with 6 serial dilutions of antimicrobial agent, Ceftriaxone (64 µg mL<sup>-1</sup> starting concentration) against bacteria and fluconazole (512 µg mL<sup>-1</sup> starting concentration).

All assays were performed in triplicate. For each triplicate, the same microbial suspension of known titer was used, inocula were quantified by determination of viable colonies upon agar plate method. The minimum inhibitory concentration (MIC) index determination was performed following the protocol CLSI-M7, modified for visually observing the growth of viable colonies on the agar surface. MIC was defined as the lowest concentration of the compounds that inhibits visible growth of the microorganism after incubation. The compounds were tested at serial dilutions factor 2, each concentration of the triplicate gave the same result in terms of microbial growth.

**Tests on Crops in a Greenhouse:** Tests on crops in the field. Test was conducted at Az. Agr. Vallese Alessandro (via Roma, 709-64014 Martinsicuro (TE)-ITALY) and at Centro Ricerche Agronomiche ed Ambientali, Res Agraria srl (via A. Canova 19/2, 64 018 Tortoreto Lido (TE)-ITALY). The trial was conducted in the field (48 plots, 28 plants/plot) by using “Kero” variety of processing tomato against *Rhizoctonia solani*. Tested compounds were used by foliar application. UPM Solargo 100 was appropriately used at different dilutions in order to have stable and sprayable liquid solutions (see Table S4, Supporting Information). The final concentration of lignin in the formulations was 100 g L<sup>-1</sup>. Commercial copper-based pesticides were used as reference control: CuCl<sub>2</sub>·3Cu(OH)<sub>2</sub> (Coprantol WG, 32% of copper) purchased by Syngenta and CuSO<sub>4</sub>·5 H<sub>2</sub>O (25% of copper) purchased by Manica. The dosage applied of Coprantol WG and CuSO<sub>4</sub>·5 H<sub>2</sub>O was 165 and 200 g ha<sup>-1</sup>, respectively, in order to have the same quantity of copper (50 g ha<sup>-1</sup>) applied per hectare in both cases. The spray volume was 800 L ha<sup>-1</sup>. Experimental conditions, crop details, and application schedules are detailed in Tables S3 and S4 (Supporting Information). The following parameters were evaluated: percentage of attacked plants (incidence) and average attacked area per plant (severity) in the field, yield per plot at harvest, vigor of plants, content of chlorophyll, water, and nitrogen on leaves. A preventive application (application A) of tested compounds was carried out and the following six applications (applications B-G) were performed with about 7–8 days of interval (Table S4, Supporting Information). A good level of disease was assessed on the trial area; an artificial inoculation of *Rhizoctonia solani* was made 10 days after the first application and 10 days after the third application. The first signs of diseases occurred 7 days after the first application and the following artificial inoculations contributed to the natural disease infection and development which reached a high level of attack during the trial period until about 43% of incidence and 30% of severity on the last assessment, 14 days after the last application. The selectivity and efficacy assessments on *Rhizoctonia solani* were made 7 days after (7 DA) each application and also 14 days (14 DA) after the last application. In Table S5 (Supporting Information) results in term of % of incidence and severity are reported for the assessments 7DA-A, 7DA-D, 7 DA-G, and 14 DA-G. Statistical analyses were applied to the incidence and severity values compared to the untreated control. For each assessment date the homogeneity of variance was tested by Levene’s test.

## Supporting Information

Supporting Information is available from the Wiley Online Library or from the author.

## Acknowledgements

This work has benefited from the equipment and framework of the COMP-HUB Initiative, funded by the “Departments of Excellence” program of the Italian Ministry for Education, University and Research (No. MIUR, 2018–2022). The authors thank Laboratorio di Strutturistica “Mario Nardelli,” University of Parma, for diffraction analyses. The authors are grateful to Dr. Monica Maffini (University of Parma) for technical assistance.

Open access funding provided by Università degli Studi di Parma within the CRUI-CARE Agreement.

## Conflict of Interest

The authors declare no conflict of interest.

## Data Availability Statement

The data that support the findings of this study are available from the corresponding author upon reasonable request.

## Keywords

antimicrobial, Cu<sub>2</sub>O, cuprite, lignin, pesticides

Received: March 7, 2022

Revised: April 22, 2022

Published online:

- [1] R. A. Festa, D. J. Thiele, *Curr. Biol.* **2011**, *21*, R877.
- [2] A. K. Boal, A. C. Rosenzweig, *Chem. Rev.* **2009**, *109*, 4760.
- [3] T. Oku, R. Motoyoshi, A. Suzuki, K. Kikuchi, S. Kikuchi, B. Jeyadevan, J. Cuya, *Adv. Mater. Sci. Eng.* **2010**, *2010*, 562842.
- [4] J. F. George, *Agric. Hist.* **1935**, *9*, 67.
- [5] J. R. Lamichhane, E. Osdaghi, F. Behlau, J. Köhl, J. B. Jones, J.-N. Aubertot, *Agron. Sustainable Dev.* **2018**, *38*, 28.
- [6] "Agri-environmental indicator – consumption of pesticides," [https://ec.europa.eu/eurostat/statistics-explained/index.php?title=Agri-environmental\\_indicator\\_-\\_consumption\\_of\\_pesticides](https://ec.europa.eu/eurostat/statistics-explained/index.php?title=Agri-environmental_indicator_-_consumption_of_pesticides) (accessed: November 2020).
- [7] O. Menkissoglu, *Phytopathology* **1991**, *81*, 1263.
- [8] P. Arman, R. L. Wain, *Ann. Appl. Biol.* **1958**, *46*, 366.
- [9] L. van Z. G. Merrington, S. L. Rogers, *Aust. J. Soil Res.* **2002**, *40*, 749.
- [10] A. K. Alva, J. H. Graham, C. A. Anderson, *Soil Sci. Soc. Am. J.* **1995**, *59*, 481.
- [11] A. K. Alva, B. Zhu, *Soil Sci. Soc. Am. J.* **1993**, *57*, 723.
- [12] European Food Safety Authority (EFSA), M. Arena, D. Auteri, S. Barmaz, G. Bellisai, A. Brancato, D. Brocca, L. Bura, H. Byers, A. Chiusolo, D. Court Marques, F. Crivellente, C. De Lentdecker, M. Egsmose, Z. Erdos, G. Fait, L. Ferreira, M. Goumenou, L. Greco, A. Ippolito, F. Istace, S. Jarrah, D. Kardassi, R. Leuschner, C. Lythgo, J. O. Magrans, P. Medina, I. Miron, T. Molnar, A. Nougadere, L. Padovani, et al., *EFSA J.* **2018**, *16*, 5152.
- [13] A. Waris, M. Din, A. Ali, M. Ali, S. Afridi, A. Baset, A. Ullah Khan, *Inorg. Chem. Commun.* **2021**, *123*, 108369.
- [14] E. Sánchez-López, D. Gomes, G. Esteruelas, L. Bonilla, A. L. Lopez-Machado, R. Galindo, A. Cano, M. Espina, M. Ettchetto, A. Camins, A. M. Silva, A. Durazzo, A. Santini, M. L. Garcia, E. B. Souto, *Nanomaterials* **2020**, *10*, 292.
- [15] R. C. Kasana, N. R. Panwar, R. K. Kaul, P. Kumar, *Environ. Chem. Lett.* **2017**, *15*, 233.
- [16] M. Vincent, P. Hartemann, M. Engels-Deutsch, *Int. J. Hyg. Environ. Health* **2016**, *219*, 585.
- [17] Y. N. Slavin, J. Asnis, U. O. Häfeli, H. Bach, *J. Nanobiotechnology* **2017**, *15*, 65.
- [18] S. Meghana, P. Kabra, S. Chakraborty, N. Padmavathy, *RSC Adv.* **2015**, *5*, 12293.
- [19] S. L. Warnes, V. Caves, C. W. Keevil, *Environ. Microbiol.* **2012**, *14*, 1730.
- [20] J. Lee, S. Mahendra, P. J. Alvarez, *ACS Nano* **2010**, *4*, 3580.
- [21] C. Bai, M. Tang, *J. Appl. Toxicol.* **2020**, *40*, 37.
- [22] A. M. Schrand, M. F. Rahman, S. M. Hussain, J. J. Schlager, D. A. Smith, A. F. Syed, *Wiley Interdiscip. Rev. Nanomed. Nanobiotechnol.* **2010**, *2*, 544.
- [23] T. Ameh, C. M. Sayes, *Environ. Toxicol. Pharmacol.* **2019**, *71*, 103220.
- [24] F. Ameen, K. Alsamhary, J. A. Alabdullatif, S. ALNadhari, *Ecotoxicol. Environ. Saf.* **2021**, *213*, 112027.
- [25] R. P. Singh, R. Handa, G. Manchanda, *J. Controlled Release* **2021**, *329*, 1234.
- [26] V. Sinisi, P. Pelagatti, M. Carcelli, A. Migliori, L. Mantovani, L. Righi, G. Leonardi, S. Pietarinen, C. Hubsch, D. Rogolino, *ACS Sustainable Chem. Eng.* **2019**, *7*, 3213.
- [27] C. Gazzurelli, A. Migliori, P. P. Mazzeo, M. Carcelli, S. Pietarinen, G. Leonardi, A. Pandolfi, D. Rogolino, P. Pelagatti, *ACS Sustainable Chem. Eng.* **2020**, *8*, 14886.
- [28] V. Martínez, M. Mitjans, M. Vinardell, *Curr. Org. Chem.* **2012**, *16*, 1863.
- [29] X. Dong, M. Dong, Y. Lu, A. Turley, T. Jin, C. Wu, *Ind. Crops Prod.* **2011**, *34*, 1629.
- [30] M. H. Sipponen, H. Lange, C. Crestini, A. Henn, M. Österberg, *ChemSusChem* **2019**, *12*, 2039.
- [31] T. M. Budnyak, A. Slabon, M. H. Sipponen, *ChemSusChem* **2020**, *13*, 4344.
- [32] O. Gordobil, R. Herrera, M. Yahyaoui, S. Ilk, M. Kaya, J. Labidi, *RSC Adv.* **2018**, *8*, 24525.
- [33] M. P. Vinardell, M. Mitjans, *Int. J. Mol. Sci.* **2017**, *18*, 1219.
- [34] M. P. Vinardell, V. Ugartondo, M. Mitjans, *Ind. Crops Prod.* **2008**, *27*, 220.
- [35] J. L. Espinoza-Acosta, P. I. Torres-Chávez, B. Ramírez-Wong, C. M. López-Saiz, B. Montañaño-Leyva, *BioResources* **2016**, *11*, 5452.
- [36] S. Hu, Y. Lo Hsieh, *Int. J. Biol. Macromol.* **2016**, *82*, 856.
- [37] S. Hu, Y. Lo Hsieh, *Carbohydr. Polym.* **2015**, *131*, 134.
- [38] S. Chandna, N. S. Thakur, Y. N. Reddy, R. Kaur, J. Bhaumik, *ACS Biomater. Sci. Eng.* **2019**, *5*, 3212.
- [39] M. J. Rak, T. Friščič, A. Moores, *Faraday Discuss.* **2014**, *170*, 155.
- [40] P. Li, W. Lv, S. Ai, *J. Exp. Nanosci.* **2016**, *11*, 18.
- [41] A. H. Zittlau, Q. Shi, J. Boerio-Goates, B. F. Woodfield, J. Majzlan, *Chem. Erde* **2013**, *73*, 39.
- [42] P. Widsten, B. Hortling, K. Poppius-Levlin, *Wood Res. Technol. Holzforsch.* **2004**, *58*, 363.
- [43] CLSI, *Methods for Dilution Antimicrobial Susceptibility Tests for Bacteria That Grow Aerobically*, 11th ed., CLSI document M07-A10, Clinical and Laboratory Standards Institute, Wayne, PA **2018**.